LETTERS
PUBLISHED ONLINE: 28 JUNE 2009 | DOI: 10.1038/NNANO.2009.156
nature nanotechnology

Determination of protein structural flexibility by microsecond force spectroscopy

Mingdong Dong, Sudhir Husale and Ozgur Sahin*

Proteins are dynamic molecular machines having structural flexibility that allows conformational changes[1,2]. Current methods for the determination of protein flexibility rely mainly on the measurement of thermal fluctuations and disorder in protein conformations[3–5] and tend to be experimentally challenging. Moreover, they reflect atomic fluctuations on picosecond timescales, whereas the large conformational changes in proteins typically happen on micro- to millisecond timescales[6,7]. Here, we directly determine the flexibility of bacteriorhodopsin—a protein that uses the energy in light to move protons across cell membranes—at the microsecond timescale by monitoring force-induced deformations across the protein structure with a technique based on atomic force microscopy. In contrast to existing methods, the deformations we measure involve a collective response of protein residues and operate under physiologically relevant conditions with native proteins.

The two-way coupling between protein chemistry and mechanics demands an understanding of the local flexibility of the protein structure so that a more accurate structure–function relationship can be established[8]. Atomic force microscope (AFM) based force spectroscopy is routinely used for mechanical property measurements of biological samples and exploring energy landscapes of proteins by stretching and unfolding single molecules[9–12]. However, the native conformations of proteins span an infinitesimal fraction of their entire configuration space. Therefore, probing the flexibility of proteins in their native conformation requires constraining the deformations in the protein structure to a few angstroms.

Recently, specially designed torsional harmonic cantilevers (THC) have been developed to perform high-speed force spectroscopic measurements while scanning the surface in tapping-mode AFM[13]. Owing to the offset location of the sharp tip seen in Fig. 1a, the torsional vibrations of this cantilever are sensitive to the forces on the vertically oscillating tip. To enable operation of this method in liquids with forces gentle enough to investigate proteins, we have redesigned the cantilever geometry and reduced its flexural and torsional force constants. Hereafter, we will refer to this new design as an L-THC (liquid torsional harmonic cantilever). Vibration spectra recorded in aqueous buffer (shown in Fig. 1b) demonstrate the ability of the torsional mode to enhance harmonic signals in liquids. Multifrequency excitation and detection of cantilever vibrations have proven to improve spatial resolution of imaging in liquid environments[14,15]. The advantage of the enhancement of multiple harmonic signals with the L-THC is the ability to recover the tip–sample force waveforms shown in Fig. 1c, which provide high-speed force–distance curves and allow specific material properties to be measured with high spatial resolution. Note that the entire period of the tip–sample force waveform in Fig. 1c is ~130 μs and the interactions span 20 μs. Furthermore, the waveform exhibits an rms. force noise of ~10 pN. This represents more than three orders of magnitude improvement in force sensitivity compared to the measurements performed with conventional cantilevers in liquid[16]. This advance enabled a reduction in the peak interaction forces to allow investigations of various types of proteins without causing them to be denatured. In addition, owing to the microsecond duration of force loading, the mechanical properties derived from these waveforms will reflect molecular behaviour at the microsecond timescale. We therefore refer to these mechanical measurements as microsecond force spectroscopy.

We have investigated the flexibility of bacteriorhodopsin (bR), a light-driven proton pump forming the purple membranes of *Halobacterium salinarum*[17]. bR goes through large conformational changes during its photochemical cycle[6,7], and is responsible for controlling proton conduction from the cytoplasm to the active site of the protein containing retinal[18]. Measurements of force-induced deformations on both the cytoplasmic and extracellular sides of the purple membrane with our AFM-based technique can help determine the flexibility of bR, as well as the lipids surrounding them.

Using the L-THC we scanned purple membrane patches adsorbed onto a mica substrate in the tapping mode and generated topography, phase and flexibility maps, simultaneously. Figure 2a shows a tapping-mode topography image of two adjacent membrane patches. The corresponding height profile in Fig. 2f reveals different apparent thicknesses for these membranes of 5.7 and 7.2 nm, respectively. This contrast, manifested by the effect of electrostatic interactions[19], allows the cytoplasmic and extracellular surfaces to be distinguished[20]. The higher surface charge of the cytoplasmic side leads to an increased apparent height as observed with the membrane patch on the top side of Fig. 2a. The phase image, which is conventionally known to be sensitive to material contrast, does not show any noticeable differences between the two adjacent patches (Fig. 2b,g).

We generated the flexibility map by analysing the high-speed force–distance curves obtained at each pixel during the tapping-mode imaging process. Local reduced elastic modulus values are approximated by fitting these curves against a contact mechanics model (see Methods). The flexibility map in Fig. 2c exhibits a surprisingly clear contrast between the membrane patches. The numerical values plotted in Fig. 2h show that the reduced elastic modulus of the extracellular side is nominally 35 MPa, whereas the cytoplasmic side is measured to be 7 MPa. The accuracies of these values are primarily limited by the accuracy of cantilever spring constant calibration[21], which can introduce an error on the order of 10%. In addition, the data in Fig. 2 h show that the elastic modulus values recorded on the extracellular and cytoplasmic sides range between 15–50 MPa and 4–10 MPa, respectively. This variation is both related to the noise in force measurements and the heterogeneity in mechanical properties of lipids and proteins.

To observe molecular details in the flexibility map, we have analysed the two patches with higher resolution. Figure 2d,e presents flexibility maps obtained by scanning regions marked with 'CP'

Rowland Institute at Harvard, Harvard University, Cambridge, Massachusetts 02142 USA. *e-mail: sahin@rowland.harvard.edu

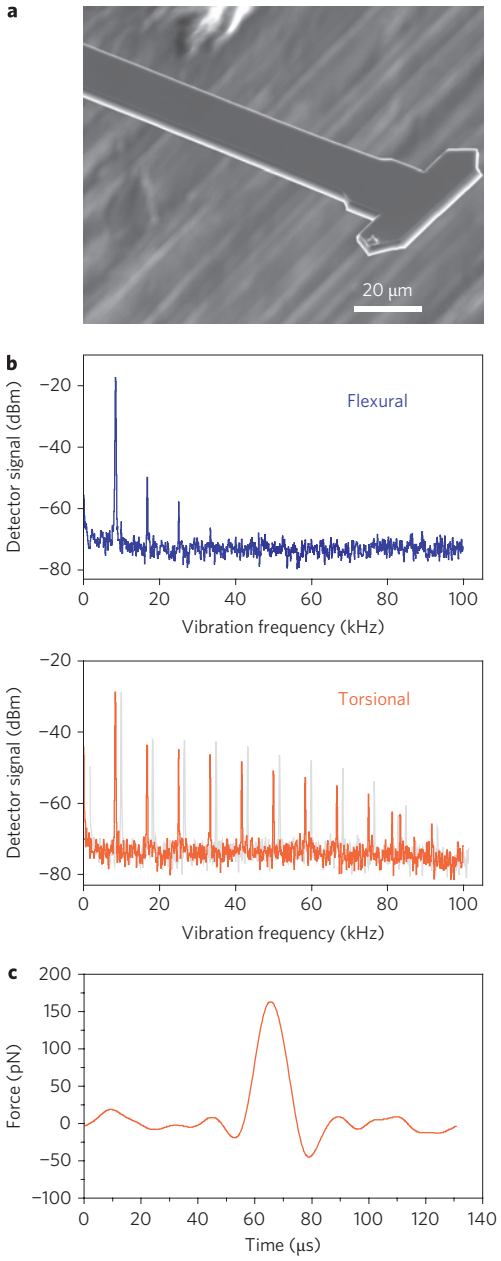

Figure 1 | Microsecond force spectroscopy in liquids. a, A scanning electron micrograph (SEM) image of a liquid torsional harmonic cantilever (L-THC). **b**, Flexural and torsional vibration spectra of an L-THC tapping on a purple membrane sample in aqueous buffer. A torsional spectrum on a mica sample is shown in light grey to show the differences in the magnitudes of high-frequency peaks in the different materials. For clarity, the spectrum on mica is offset by 2 kHz to the right. **c**, A tip–sample force waveform recovered from the torsional vibrations.

and 'EC' in Fig. 2c. Both images resolve the bR trimers arranged in a hexagonal lattice with ~6 nm spacing. The triangular morphologies of the trimers are also visible. The regions between the trimers, occupied by lipids, exhibit reduced elastic moduli lower than the proteins. The elastic modulus values recorded on the lipid regions are approximately 5 MPa on the cytoplasmic side and 16 MPa on the extracellular side. The higher value for the lipids on the extracellular side is likely a consequence of the lateral interactions coupling from the stiffer protein regions on the same side of the membrane. We believe the resolution of these measurements is limited by the relatively high spring constant of the L-THC (0.18 N m^{-1}) compared to typical values for conventional cantilevers used in fluid tapping mode.

In the above analysis of the flexibility images, we reduced the rich tip–sample interaction to a single elastic modulus parameter. The reliability of this parameter is limited by the applicability of continuum models that predict force–distance relationships between macroscopic objects in contact. Non-uniformities and voids[22] in the protein architecture or gaps between the membrane and the solid support can have a considerable effect on the measured flexibilities. In addition, surface roughness can result in changes in contact areas, which also influences phase images[23].

One can reach a better and more detailed understanding of local flexibility as well as other molecular interactions by investigating the complete force–distance curves, because interaction components such as van der Waals forces, screened electrostatic interactions and mechanical restoration forces have different spatial dependencies. Figure 3a presents force–distance curves that belong to the two sides of the purple membrane and mica. We have divided the graph into three regions to illustrate where the tip and sample are separated (I), and where they are interacting through long-range (II) and short-range forces (III). The buffer conditions used in this experiment lead to repulsive electrostatic forces on each sample with a screening length of ~0.55 nm. Therefore, region II reveals a competition between the attractive van der Waals forces and repulsive electrostatic forces. We see that the forces measured on each sample in this region follow the same order of surface charge densities expected from these samples, that is, from high to low: cytoplasmic side, extracellular side and mica[20,24].

The information regarding the local flexibility of the sample resides in region III of Fig. 3a where the tip is in direct contact with the sample. The repulsive interaction forces lead to angstrom-scale deformations in the sample surface, which have been visualized by the topographical images in contact-mode AFM[25,26]. In this interaction region, the variation of tip–sample forces is determined mainly by the local flexibility of the sample. In fact, the short-range nature of these mechanical restoration forces makes it possible to generate flexibility maps with high spatial resolution as seen in Fig. 2d,e. One can describe local flexibility in a simpler way with effective force constants that can be obtained from the slopes of the curves in region III. From the data in Fig. 3a we obtained 0.13 N m^{-1} for the cytoplasmic side, 0.39 N m^{-1} for the extracellular side and 2.25 N m^{-1} for the mica substrate.

We carried out additional flexibility measurements on the two sides of the purple membranes under different buffer conditions. Although measurements in buffers with 300 mM and 1 M salt (KCl) concentrations at a constant pH of 7.8 did not show noticeable differences in stiffness, changing the pH of the imaging buffer resulted in changes in the effective force constants. Table 1 shows average force constants and their variation observed on each region of the sample at three pH levels. From the data we see that the apparent stiffnesses on either side of the membrane slightly increase with increasing pH and that the stiffness contrast is more dramatic at pH 6 (flexibility maps and force–distance curves for these measurements are provided in the Supplementary Information). The pH-dependent analysis of effective force constants reflects the utility of our AFM-based approach in that it allows probing of the flexibility of membrane proteins in a range of biologically relevant conditions.

The differentiation of the flexibility of cytoplasmic and extracellular sides and the nanometre-scale lateral resolution observed in the flexibility maps are enabled by the confinement of mechanical interactions to the vicinity of the contact region in AFM, as illustrated in Fig. 3b. The measured flexibility is therefore determined predominantly by the collective response of the protein residues and lipids within this interacting volume. The observed flexibility contrast